LILIAN COELHO DE FREITAS
(ORGANIZADORA)

Collection:

APPLIED COMPUTER ENGINEERING

Atena Editora
Ano 2022

LILIAN COELHO DE FREITAS
(ORGANIZADORA)

Collection:

APPLIED COMPUTER ENGINEERING

Atena Editora
Ano 2022

Editora chefe
Profª Drª Antonella Carvalho de Oliveira
Editora executiva
Natalia Oliveira
Assistente editorial
Flávia Roberta Barão
Bibliotecária
Janaina Ramos
Projeto gráfico
Camila Alves de Cremo
Daphynny Pamplona
Gabriel Motomu Teshima
Luiza Alves Batista
Natália Sandrini de Azevedo
Imagens da capa
iStock
Edição de arte
Luiza Alves Batista

2022 *by Atena Editora*
Copyright © Atena Editora
Copyright do texto © 2022 Os autores
Copyright da edição © 2022 Atena Editora
Direitos para esta edição cedidos à Atena Editora pelos autores.
Open access publication by Atena Editora

Todo o conteúdo deste livro está licenciado sob uma Licença de Atribuição *Creative Commons*. Atribuição-Não-Comercial-NãoDerivativos 4.0 Internacional (CC BY-NC-ND 4.0).

O conteúdo dos artigos e seus dados em sua forma, correção e confiabilidade são de responsabilidade exclusiva dos autores, inclusive não representam necessariamente a posição oficial da Atena Editora. Permitido o *download* da obra e o compartilhamento desde que sejam atribuídos créditos aos autores, mas sem a possibilidade de alterá-la de nenhuma forma ou utilizá-la para fins comerciais.

Todos os manuscritos foram previamente submetidos à avaliação cega pelos pares, membros do Conselho Editorial desta Editora, tendo sido aprovados para a publicação com base em critérios de neutralidade e imparcialidade acadêmica.

A Atena Editora é comprometida em garantir a integridade editorial em todas as etapas do processo de publicação, evitando plágio, dados ou resultados fraudulentos e impedindo que interesses financeiros comprometam os padrões éticos da publicação. Situações suspeitas de má conduta científica serão investigadas sob o mais alto padrão de rigor acadêmico e ético.

Conselho Editorial
Ciências Exatas e da Terra e Engenharias
Prof. Dr. Adélio Alcino Sampaio Castro Machado – Universidade do Porto
Profª Drª Alana Maria Cerqueira de Oliveira – Instituto Federal do Acre
Profª Drª Ana Grasielle Dionísio Corrêa – Universidade Presbiteriana Mackenzie
Profª Drª Ana Paula Florêncio Aires – Universidade de Trás-os-Montes e Alto Douro
Prof. Dr. Carlos Eduardo Sanches de Andrade – Universidade Federal de Goiás
Profª Drª Carmen Lúcia Voigt – Universidade Norte do Paraná

Atena Editora
Ano 2022

Prof. Dr. Cleiseano Emanuel da Silva Paniagua – Instituto Federal de Educação, Ciência e Tecnologia de Goiás
Prof. Dr. Douglas Gonçalves da Silva – Universidade Estadual do Sudoeste da Bahia
Prof. Dr. Eloi Rufato Junior – Universidade Tecnológica Federal do Paraná
Profª Drª Érica de Melo Azevedo – Instituto Federal do Rio de Janeiro
Prof. Dr. Fabrício Menezes Ramos – Instituto Federal do Pará
Profª Dra. Jéssica Verger Nardeli – Universidade Estadual Paulista Júlio de Mesquita Filho
Prof. Dr. Juliano Bitencourt Campos – Universidade do Extremo Sul Catarinense
Prof. Dr. Juliano Carlo Rufino de Freitas – Universidade Federal de Campina Grande
Profª Drª Luciana do Nascimento Mendes – Instituto Federal de Educação, Ciência e Tecnologia do Rio Grande do Norte
Prof. Dr. Marcelo Marques – Universidade Estadual de Maringá
Prof. Dr. Marco Aurélio Kistemann Junior – Universidade Federal de Juiz de Fora
Prof. Dr. Miguel Adriano Inácio – Instituto Nacional de Pesquisas Espaciais
Profª Drª Neiva Maria de Almeida – Universidade Federal da Paraíba
Profª Drª Natiéli Piovesan – Instituto Federal do Rio Grande do Norte
Profª Drª Priscila Tessmer Scaglioni – Universidade Federal de Pelotas
Prof. Dr. Sidney Gonçalo de Lima – Universidade Federal do Piauí
Prof. Dr. Takeshy Tachizawa – Faculdade de Campo Limpo Paulista

Atena
Editora
Ano 2022

Collection: applied computer engineering

Diagramação: Camila Alves de Cremo
Correção: Yaiddy Paola Martinez
Indexação: Amanda Kelly da Costa Veiga
Revisão: Os autores
Organizadora: Lilian Coelho de Freitas

Dados Internacionais de Catalogação na Publicação (CIP)

C697 Collection: applied computer engineering / Organizadora Lilian Coelho de Freitas. – Ponta Grossa - PR: Atena, 2022.

Formato: PDF
Requisitos de sistema: Adobe Acrobat Reader
Modo de acesso: World Wide Web
Inclui bibliografia
ISBN 978-65-5983-859-2
DOI: https://doi.org/10.22533/at.ed.592222801

1. Computer engineering. I. Freitas, Lilian Coelho de (Organizadora). II. Título.

CDD 621.39

Elaborado por Bibliotecária Janaina Ramos – CRB-8/9166

Atena Editora
Ponta Grossa – Paraná – Brasil
Telefone: +55 (42) 3323-5493
www.atenaeditora.com.br
contato@atenaeditora.com.br

Atena Editora
Ano 2022

DECLARAÇÃO DOS AUTORES

Os autores desta obra: 1. Atestam não possuir qualquer interesse comercial que constitua um conflito de interesses em relação ao artigo científico publicado; 2. Declaram que participaram ativamente da construção dos respectivos manuscritos, preferencialmente na: a) Concepção do estudo, e/ou aquisição de dados, e/ou análise e interpretação de dados; b) Elaboração do artigo ou revisão com vistas a tornar o material intelectualmente relevante; c) Aprovação final do manuscrito para submissão.; 3. Certificam que os artigos científicos publicados estão completamente isentos de dados e/ou resultados fraudulentos; 4. Confirmam a citação e a referência correta de todos os dados e de interpretações de dados de outras pesquisas; 5. Reconhecem terem informado todas as fontes de financiamento recebidas para a consecução da pesquisa; 6. Autorizam a edição da obra, que incluem os registros de ficha catalográfica, ISBN, DOI e demais indexadores, projeto visual e criação de capa, diagramação de miolo, assim como lançamento e divulgação da mesma conforme critérios da Atena Editora.

DECLARAÇÃO DA EDITORA

A Atena Editora declara, para os devidos fins de direito, que: 1. A presente publicação constitui apenas transferência temporária dos direitos autorais, direito sobre a publicação, inclusive não constitui responsabilidade solidária na criação dos manuscritos publicados, nos termos previstos na Lei sobre direitos autorais (Lei 9610/98), no art. 184 do Código Penal e no art. 927 do Código Civil; 2. Autoriza e incentiva os autores a assinarem contratos com repositórios institucionais, com fins exclusivos de divulgação da obra, desde que com o devido reconhecimento de autoria e edição e sem qualquer finalidade comercial; 3. Todos os e-book são *open access, desta forma* não os comercializa em seu site, sites parceiros, plataformas de *e-commerce,* ou qualquer outro meio virtual ou físico, portanto, está isenta de repasses de direitos autorais aos autores; 4. Todos os membros do conselho editorial são doutores e vinculados a instituições de ensino superior públicas, conforme recomendação da CAPES para obtenção do Qualis livro; 5. Não cede, comercializa ou autoriza a utilização dos nomes e e-mails dos autores, bem como nenhum outro dado dos mesmos, para qualquer finalidade que não o escopo da divulgação desta obra.

Atena
Editora
Ano 2022

APRESENTAÇÃO

Atena Editora is honored to present the e-book entitled "*Collection: Applied Computer Engineering*". This volume presents 17 chapters about applications of computer engineering in industrial automation, robotics, data science, information security, neuromarketing, speech development in children, among others.

We want to take this moment to thank all of our authors for entrusting us with their discoveries. We are also grateful to the reviewers and readers who have contributed to the success of our books.

Enjoy your reading.

Lilian Coelho de Freitas

SUMÁRIO

CAPÍTULO 1 1

ALIMENTADOR AUTOMÁTICO DE PET UTILIZANDO A PLATAFORMA ARDUÍNO

Márcio Valério de Oliveira Favacho
Vivian da Silva Lobato
Raphael Saraiva de Sousa
Alberto Cauã Trindade da Silva
Denise Nascimento Cardoso
Jamilly da Silva Dias
Jéssica Ferreira e Ferreira
Pedro Afonso Alcântara Negrão
Rízia de Cássia da Fonseca Pereira
Ruam Melo dos Santos
Weliton Quaresma Ferreira

https://doi.org/10.22533/at.ed.5922228011

CAPÍTULO 2 14

ANÁLISE DE AGRUPAMENTO PARA APRIMORAR A EXTRAÇÃO AUTOMÁTICA DE DEMONSTRATIVOS FINANCEIROS COM ESTUDO DE ESCALABILIDADE

Igor Raphael Magollo
Gabriel Olivato
Victor Vieira Ferraz
Murilo Coelho Naldi

https://doi.org/10.22533/at.ed.5922228012

CAPÍTULO 3 32

AVALIANDO A USABILIDADE DE APLICAÇÕES VOLTADAS PARA A COMUNICAÇÃO DE CRIANÇAS COM TEA

Joêmia Leilane Gomes de Medeiros
Welliana Benevides Ramalho
Edinadja Mayara de Macedo

https://doi.org/10.22533/at.ed.5922228013

CAPÍTULO 4 47

CONTROLE E MONITORAMENTO AUTOMATIZADO DOS FATORES LIMNOLÓGICOS IDEAIS PARA LARVICULTURA DO PTEROPHYLLUM SCALARE (ACARÁ BANDEIRA) UTILIZANDO TÉCNICAS DE INTELIGÊNCIA ARTIFICAL

Raphael Saraiva de Sousa
Otávio Noura Teixeira
Augusto César Paes de Souza
Márcio Valério de Oliveira Favacho
Renato Hidaka Torres

https://doi.org/10.22533/at.ed.5922228014

CAPÍTULO 5 63

GESTIÓN DE RIESGOS Y CONTINUIDAD DEL NEGOCIO SOBRE LA SEGURIDAD

INFORMÁTICA EN EL SECTOR RETAIL EN MÉXICO
José Eduardo Mendoza Macias
Emigdio Larios Gómez
https://doi.org/10.22533/at.ed.5922228015

CAPÍTULO 6.....73

IAÇÁ – OTIMIZAÇÃO DO PROCESSO DE EXTRAÇÃO DA POLPA DE AÇAÍ UTILIZANDO A PLATAFORMA ARDUÍNO
Márcio Valério de Oliveira Favacho
Vivian da Silva Lobato
Adenildo da Conceição Silva da Silva
Ana Flavia Dias da Silva
Ian Castro Marinho da Silva
Leonan Gustavo Silva Rodrigues
Lilian Raquel de Campos Cardoso
Marily Luciene Pantoja Costa
Nayra Pereira Ferreira
Paulo Vitor Melo Amaral Ferreira
Rodrigo Figueiró Santana
https://doi.org/10.22533/at.ed.5922228016

CAPÍTULO 7.....84

LINGUAGEM DE DOMÍNIO ESPECÍFICO PARA A AUTORIA DE APLICAÇÕES PARA TV DIGITAL
Lucas de Macedo Terças
Daniel de Sousa Moraes
Carlos de Salles Soares Neto
https://doi.org/10.22533/at.ed.5922228017

CAPÍTULO 8.....95

NEUROMARKETING APLICADO AO EMOCIONAL BRANDING
Maiara Bettu
Vanessa Angélica Balestrin
https://doi.org/10.22533/at.ed.5922228018

CAPÍTULO 9..... 111

PROPOSTA DE METAMODELOS DE GEOVISUALIZAÇÃO COM RECURSOS ADAPTÁVEIS
Ítalo Moreira Silva
Alexandre Carvalho Silva
Camilo de Lellis Barreto Junior
Diogo Aparecido Cavalcante de Lima
https://doi.org/10.22533/at.ed.5922228019

CAPÍTULO 10.....116

SISTEMA INTEGRAL AUTOMATIZADO DE SEGUIMIENTO DE EGRESADOS Y

EMPLEADORES
Leonor Angeles Hernández
Mónica Leticia Acosta Miranda
Daniel Domínguez Estudillo
Edi Ray Zavaleta Olea
José Arnulfo Corona Calvario
https://doi.org/10.22533/at.ed.59222280110

CAPÍTULO 11 126

STRENGTH PREDICTION OF ADHESIVELY-BONDED JOINTS WITH COHESIVE LAWS ESTIMATED BY DIGITAL IMAGE CORRELATION
Ulisses Tiago Ferreira Carvalho
Raul Duarte Salgueiral Gomes Campilho
https://doi.org/10.22533/at.ed.59222280111

CAPÍTULO 12 140

TAGARELAPP: PROTÓTIPO DE INTERFACE CENTRADO NA USABILIDADE PARA O DESENVOLVIMENTO DA FALA E COMUNICAÇÃO DE CRIANÇAS COM TEA
Joêmia Leilane Gomes de Medeiros
Welliana Benevides Ramalho
Edinadja Mayara de Macedo
https://doi.org/10.22533/at.ed.59222280112

CAPÍTULO 13 152

ESTRATEGIA DE MIGRACIÓN DE UN SISTEMA LEGADO UTILIZANDO LA METODOLOGÍA “CHICKEN LITTLE” APLICADA AL SISTEMA DE BEDELÍAS DE LA UNIVERSIDAD DE LA REPÚBLICA DE URUGUAY
Cristina González
Mariela De León
https://doi.org/10.22533/at.ed.59222280113

CAPÍTULO 14 169

INTRODUÇÃO A ANÁLISE FORENSE COMPUTACIONAL: DETECTANDO ROOTKITS EM AMBIENTE WINDOWS
Thiago Giroto Milani
Ricardo Slavov
https://doi.org/10.22533/at.ed.59222280114

CAPÍTULO 15 191

USO DAS TICS COMO METODO PARA ELABORAR TRABALHO RECEPCIONAL E PLATAFORMA PARA A AUTOMATIZAÇÃO DE FORMATOS DE ESTADIAS
Eloína Herrera Rodríguez
Sonia López Rodríguez
Claudia Galicia Solís
https://doi.org/10.22533/at.ed.59222280115

CAPÍTULO 16.....209

NARRATIVAS ACADÊMICAS EM PESQUISA: MÁQUINAS DE GUERRA VIRTUAIS

Angeli Rose

https://doi.org/10.22533/at.ed.59222280116

CAPÍTULO 17.....218

OPTIMIZATION BASED OUTPUT FEEDBACK CONTROL DESIGN IN DESCRIPTOR SYSTEMS

Elmer Rolando Llanos Villarreal
Maxwell Cavalcante Jácome
Edpo Rodrigues de Morais
João Victor de Queiroz
Walter Martins Rodrigues

https://doi.org/10.22533/at.ed.59222280117

SOBRE A ORGANIZADORA 225

ÍNDICE REMISSIVO.....226

CAPÍTULO 11

STRENGTH PREDICTION OF ADHESIVELY-BONDED JOINTS WITH COHESIVE LAWS ESTIMATED BY DIGITAL IMAGE CORRELATION

Data de aceite: 10/01/2022
Data de submissão: 08/10/2021

Ulisses Tiago Ferreira Carvalho
Instituto Superior de Engenharia do Porto, Instituto Politécnico do Porto
Porto, Portugal
ORCID: 0000-0001-8920-9297

Raul Duarte Salgueiral Gomes Campilho
Instituto Superior de Engenharia do Porto, Instituto Politécnico do Porto
Porto, Portugal
ORCID: 0000-0003-4167-4434

ABSTRACT: Cohesive Zone Models (CZM) are an accurate design method for bonded structures but, depending on the adhesive type and specimen's geometry, the accuracy of the strength predictions may be highly compromised by the choice of the cohesive laws. This work presents a validation of tensile and shear CZM laws of three adhesives obtained by the direct method applied to Double-Cantilever Beam (DCB) and End-Notched Flexure (ENF) tests, respectively. The validation is carried out by considering a mixed-mode bonded geometry (the single-lap joint) with different overlap lengths (L_O) and adhesives of distinct ductility. Initially, the precise shape of the cohesive law in tension and shear of the adhesives is estimated, followed by their simplification to parameterized triangular, trapezoidal and linear-exponential CZM laws. Validation of the CZM laws was accomplished by direct comparison of the load-displacement (P-δ) curves and maximum load (P_m) of the single-lap joints as a function of the tested L_O values. The strength predictions were accurate for a CZM law shape consistent with the adhesive type, although the differences between CZM shapes were not too significant.

KEYWORDS: Structural adhesives; Adhesive joints; Finite element method; Cohesive zone models; Digital image correlation.

PREVISÃO DE RESISTÊNCIA DE LIGAÇÕES ADESIVAS COM LEIS COESIVAS ESTIMADAS POR CORRELAÇÃO DIGITAL DE IMAGEM

RESUMO: Os modelos de dano coesivo (MDC) são um método de projeto preciso para ligações adesivas, mas, dependendo do tipo de adesivo e geometria da ligação, a precisão das previsões de resistência pode ser altamente comprometida pela escolha das leis coesivas. Este trabalho apresenta uma validação das leis MDC de tração e corte de três adesivos, obtidas pelo método direto aplicado aos ensaios *Double-Cantilever Beam* (DCB) e *End-Notched Flexure* (ENF), respetivamente. A validação é realizada com uma geometria de modo misto (a junta de sobreposição simples) com diferentes comprimentos de sobreposição (L_O) e adesivos de ductilidade distinta. Inicialmente, é estimada a forma precisa da lei coesiva em tensão e corte dos adesivos, seguida de sua simplificação para leis MDC triangulares, trapezoidais e lineares exponenciais parametrizadas. A validação das leis MDC foi realizada por comparação direta das curvas força-deslocamento (P-δ) e carga máxima

(P_m) das juntas de sobreposição simples em função dos valores de L_O testados. As previsões de resistência foram precisas para uma forma de lei MDC consistente com o tipo de adesivo, embora as diferenças entre as formas da lei MDC não fossem muito significativas.
PALAVRAS-CHAVE: Adesivos estruturais; Juntas adesivas; Método de elementos finito; Modelos de dano coesivo; Correlação digital de imagem.

1 | INTRODUCTION

Joining with structural adhesives in the aeronautical industry dates back to the 1950's, although only more recently this technique has been implemented to load bearing parts in other industries. Nowadays, adhesive bonding allows reducing the structural weight and improving performance over mechanical joints by safely enabling joining different materials and eliminating external components such as bolts or rivets, concurrently providing less sources of stress concentrations (although peak stresses usually develop at the overlap edges) (LOUREIRO *et al.*, 2010). Disadvantages are strength depreciation under conditions of bonding quality reduction, absence of techniques to detect weak or kissing bonds and in some cases inability of bonded joints to comply with certification rules (FLOROS *et al.*, 2015). The most common joint configurations are single-lap, double-lap and scarf joints. The single-lap joint is preferably considered for research and practical applications due to the ease of fabrication and generalised use in several applications. Several studies using these geometries, such as the one of AYDIN *et al.* (2005), showed the influence on strength of factors such as the adhesive thickness (t_A), adherend thickness (t_P), geometry, mechanical properties of the adherends and adhesives, and surface treatment.

Design methods for bonded joints can be either analytical or numerical. Analytical methods provide closed-form solutions for the stresses along the bondline that, together with stress or strain-based criteria, give joint strength predictions. Numerical methods overcome the simplifying assumptions' issue and, depending on the technique, may allow modelling the progressive failure of the joints by using energetic parameters such as G_C, which already revealed fundamental to model the behaviour of bonded joints. Numerical analyses are typically linked to the Finite Element Method (FEM), and they can range from the simple continuum mechanics analyses to CZM or the Extended Finite Element Method (XFEM). The main parameters of the cohesive laws, to be introduced in the numerical models, are t_n^0 and t_s^0 (cohesive strengths in tension and shear, respectively, giving the peak tractions), and the values of critical tensile and shear strain energy release rate (G_{IC} and G_{IIC}, respectively). When using CZM for strength prediction purposes, it is important that the adhesive is characterized in joints with similar geometrical conditions of the bonded structures to be simulated, and that the CZM law shape agrees with the adhesive's behaviour (CAMPILHO *et al.*, 2011). The necessary cohesive parameters (G_{IC}, G_{IIC}, t_n^0 and t_s^0) can be estimated by the property identification technique, the direct method and the inverse method. These methods usually rely on DCB or ENF tests. The fracture analysis of bonded joints should

be properly adapted, for instance considering data reduction methods that account for the modern adhesives' plasticity (CAMPILHO *et al.*, 2015). The property identification technique relies on the isolated calculation of each parameter, while in the inverse method at least one of the CZM parameters are estimated by iterative fitting the FEM prediction of the *P-d* curve with the respective experiment up to achieving a good agreement. As discussed by PANDYA and WILLIAMS (2000), the direct method provides the precise CZM shape directly from fracture tests such as the DCB or ENF, by differentiating the tensile strain energy release rate, G_I, for tension, or the shear strain energy release rate, G_{II}, for shear, with respect to δ_n or δ_s. A critical step of this technique is the measurement of δ_n or δ_s, and this can be based either on physical sensors (e.g. work of JI *et al.* (2010)) or digital image correlation (e.g. VALOROSO *et al.* (2013)). JUMEL *et al.* (2015) used the Mixed-Mode Bending (MMB) specimen and the same technique to study the fracture process of bonded joints. Peel and shear cohesive stresses in the adhesive layer were calculated by differentiation of the backface strains in tension and shear modes, respectively, while the interface displacement discontinuities were found by integrating the same quantities. After the determination of the CZM laws by the direct method, their accuracy can be checked by overlapping the numerical *P-d* curves of models using the CZM laws with the experimental *P*-δ curves from the tests (VALOROSO *et al.*, 2013). However, this validation should also comprise testing the pure mode CZM laws in a mixed-mode geometry, which is yet not available in the literature.

This work presents a validation of tensile and shear CZM laws of three adhesives obtained by the direct method applied to DCB and ENF tests, respectively. The validation is carried out by considering a mixed-mode bonded geometry (the single-lap joint) with different values of L_O and adhesives of distinct ductility. Initially, the precise shape of the cohesive law in tension and shear of the adhesives is estimated, followed by their simplification to parameterized triangular, trapezoidal and linear-exponential CZM laws. Validation of the CZM laws was accomplished by direct comparison of the *P*-δ curves and P_m of the single-lap joints as a function of the tested L_O values.

2 | EXPERIMENTAL PART

2.1 Adherends and adhesives

For the DCB, ENF and single-lap specimens, the high strength and ductile aluminium alloy AA6082 T651 was chosen for the adherends, to guarantee measurement of the CZM laws without adherend plasticization. The tensile mechanical properties of this material were obtained in the work of CAMPILHO *et al.* (2011): Young's modulus (E) of 70.07±0.83 GPa, tensile yield stress (σ_y) of 261.67±7.65 MPa, tensile failure strength (σ_f) of 324±0.16 MPa and tensile failure strain (ε_f) of 21.70±4.24%. The experimental testing programme included three structural adhesives: the brittle epoxy Araldite® AV138, the ductile epoxy Araldite® 2015 and the ductile polyurethane Sikaforce® 7752. These adhesives were previously

characterized regarding the mechanical and fracture properties (CAMPILHO *et al.*, 2013; CAMPILHO *et al.*, 2011). Bulk specimens were tested in a servo-hydraulic machine to obtain E, σ_y, σ_f and ε_f. The DCB test was selected to obtain G_{IC} and the ENF test was used for G_{IIC}. The collected data of the adhesives is summarized in Table 1.

Property	**AV138**	**2015**	**7752**
Young's modulus, E [GPa]	4.89±0.81	1.85±0.21	0.49±0.09
Poisson's ratio, v	0.35 [a]	0.33 [a]	0.30 [a]
Tensile yield stress, σ_y [MPa]	36.49±2.47	12.63±0.61	3.24±0.48
Tensile failure strength, σ_f [MPa]	39.45±3.18	21.63±1.61	11.48±0.25
Tensile failure strain, ε_f [%]	1.21±0.10	4.77±0.15	19.18±1.40
Shear modulus, G [GPa]	1.56±0.01	0.56±0.21	0.19±0.01
Shear yield stress, t_y [MPa]	25.1±0.33	14.6±1.3	5.16±1.14
Shear failure strength, t_f [MPa]	30.2±0.40	17.9±1.8	10.17±0.64
Shear failure strain, y_f [%]	7.8±0.7	43.9±3.4	54.82±6.38
G_{IC} [N/mm]	0.20 [b]	0.43±0.02	2.36±0.17
G_{IIC} [N/mm]	0.38 [b]	4.70±0.34	5.41±0.47

[a] manufacturer's data

[b] estimated in CAMPILHO *et al.* (2011)

Table 1 – Properties of the adhesives Araldite® AV138, Araldite® 2015 and Sikaforce® 7752 (CAMPILHO et al., 2013; CAMPILHO et al., 2011).

2.2 Joint geometry and testing

Fig. 1 depicts the geometry of the DCB (a) and ENF specimens (b), whose dimensions are as follows: length L=140 mm (DCB) or mid-span L=100 mm (ENF), initial crack length a_0≈50 mm, t_P=3 mm, t_A=0.2 mm and width B=25 mm.

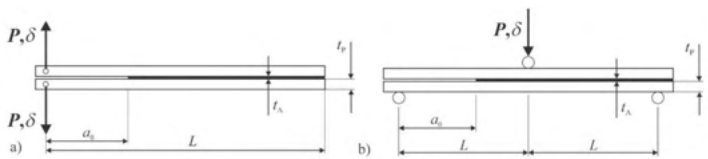

Fig. 1 – DCB (a) and ENF (b) test specimens for tensile and shear characterization of the adhesive layer, respectively.

Fig. 2 shows the geometry of the single-lap joints with the dimensions: length between grips L_T=170 mm, t_P=3 mm, t_A=0.2 mm, L_O=12,5, 25, 37.5 and 50 mm and B=25 mm (not shown in the figure).

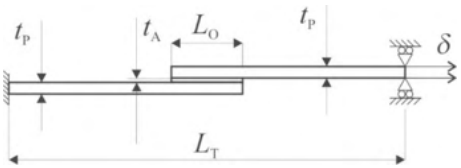

Fig. 2 – Geometry and characteristic dimensions of the single-lap joint specimens.

Testing was carried out in a Shimadzu AG-X 100 machine with a 100 kN load cell. To make possible the application of the direct method to the DCB and ENF tests (described in the following Section), 18 MPixel digital images were recorded. This enabled obtaining a, δ_n, δ_s and the adherends' rotation at the crack tip, θ_o, this last parameter required in the DCB tests for application of the J-integral. Full details of the DCB and ENF tests to obtain the CZM laws are presented in the works of CONSTANTE *et al.* (2015) and LEITÃO *et al.* (2015), respectively.

2.3 Direct method for the DCB and ENF tests

The direct formulation presented here uses the J-integral expression as basis to develop a G_I equation that can be used for the DCB test, considering the beam theory and the energetic force concept, leading to (ZHU *et al.*, 2009)

$$G_I = 12\frac{(P_u a)^2}{E_x t_P^3} + P_u\theta_o \quad \text{or} \quad G_I = P_u\theta_p. \tag{1}$$

P_u is the applied load divided by the width, E_x is the adherends' value of E in the longitudinal direction and θ_p is the rotation of the adherends where the load is applied. Fig. 3 shows the quantities δ_n, θ_o and θ_p necessary by the direct method. Also represented in the figure are δ_n^0 (relative displacement at t_n^0) and δ_n^f (tensile relative displacement at failure). The $t_n(\delta_n)$ or tensile CZM law is estimated with the differentiation of equation to the variable d_n. More details about this technique applied to the DCB specimen can be found in the work of CONSTANTE *et al.* (2015). A developed algorithm was used to measure θ_o and δ_n based on digital image correlation and tracking reference points in the scales that follow crack growth during the test.

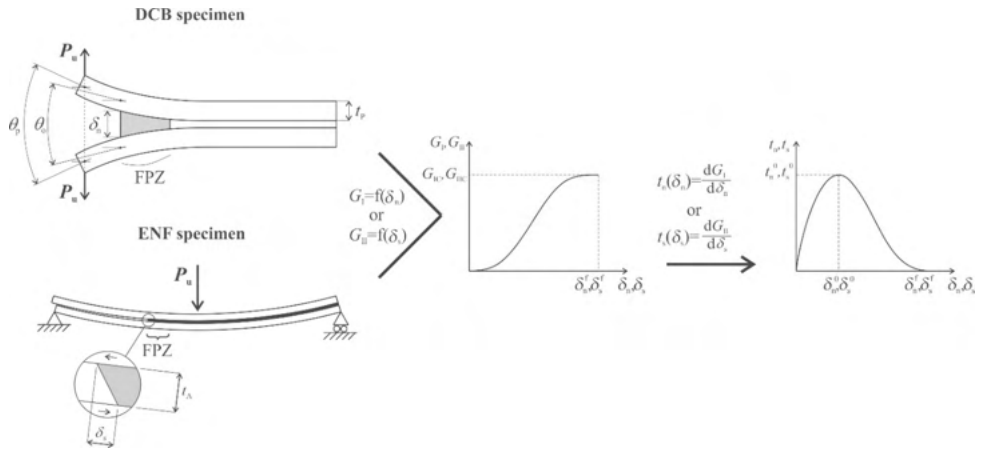

Fig. 3 – Direct method applied to the tensile and shear cohesive law estimation.

An identical procedure, i.e., based on the direct method, was used to evaluate G_{IIC} and shear CZM law by the ENF test (ZHU *et al.*, 2009), involving the concurrent measurement of the *J*-integral and δ_s (Fig. 3). The G_{II} expression for the ENF specimen was presented by LEFFLER *et al.* (2007) as

$$G_{II} = \frac{9}{16}\frac{(P_u a)^2}{E_x t_P^3} + \frac{3}{8}\frac{P_u \delta_s}{t_P}. \quad (2)$$

The t_s-δ_s curve (or shear CZM law) can then be assessed by differentiation of the G_{II}-δ_s curve. Full details regarding the description of the direct method applied to the ENF specimen, as well as the algorithm to estimate δ_s in every picture of a test, can be found in the work of LEITÃO *et al.* (2015).

3 I CZM SIMULATIONS

3.1 Underlying theory

To validate the CZM laws obtained by the direct method, approximated triangular, trapezoidal and linear-exponential laws were fit to the average experimental laws of each adhesive. Fig. 4 depicts these CZM laws with the relevant nomenclature (δ_s^0 the relative displacement at t_s^0, δ_s^f is the shear failure displacement, and δ_n^s and δ_s^s are the tensile and shear stress softening onset displacements of the trapezoidal CZM law, respectively).

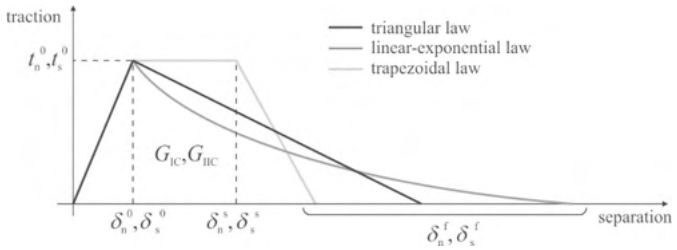

Fig. 4 – Triangular, trapezoidal and linear-exponential CZM laws.

In these laws, δ_n^f and δ_s^f are defined by making $G_I=G_{IC}$ for tension or $G_{II}=G_{IIC}$ for shear, as described by TURON *et al.* (2007). The elastic behaviour is established between the current stresses and strains in tension and shear (subscripts n and s, respectively) as

$$\mathbf{t}=\begin{Bmatrix} t_n \\ t_s \end{Bmatrix}=\begin{bmatrix} K_{nn} & K_{ns} \\ K_{ns} & K_{ss} \end{bmatrix}\cdot\begin{Bmatrix} \varepsilon_n \\ \varepsilon_s \end{Bmatrix}=\mathbf{K}\boldsymbol{\varepsilon}. \tag{3}$$

ε_n and ε_s are the tensile and shear strain, respectively. For thin adhesive layers it can be stated that $K_{nn}=E$, $K_{ss}=G$, $K_{ns}=0$ (G is the shear modulus) (CAMPILHO *et al.*, 2011). The stress depreciation portion of the laws is defined by a damage variable (d_n for tension or d_s for shear)

$$\begin{aligned} t_n &= (1-d_n)\,t_n^{\text{und}} \\ t_s &= (1-d_s)\,t_s^{\text{und}} \end{aligned}, \tag{4}$$

where t_n^{und} and t_s^{und} represent the current tensile and shear stresses, respectively if no degradation of stiffness had occurred due to softening. The damage variable takes the limit values $d_{n,s}=0$ before damage (in the elastic region) and $d_{n,s}=1$ at full degradation. The expressions for $d_{n,s}$ considering the triangular, trapezoidal and exponential laws can be found in reference (ABAQUS®, 2013). For the linear-exponential law a non-dimensional parameter*a* exists to define the rate of damage evolution with $\delta_{n,s}$ (for α=0 a triangular law is attained). In this work, α=7 was chosen.

3.2 Implementation of the model in Abaqus®

Validation of the pure-mode CZM laws obtained by the direct method was undertaken in Abaqus®, considering geometrically non-linear and two-dimensional (2D) FEM models. For the strength predictions, CZM elements were placed along the adhesive layer. The adherends were modelled as elasto-plastic using CPE4 elements and the adhesive layer's behaviour by CZM elements using a single row of elements connecting both adherends (COH2D4 4-node cohesive elements from Abaqus®) (CAMPILHO *et al.*, 2013). Fig. 5 shows the mesh details at the overlap for the L_O=12.5 mm single-lap joint. The CZM elements' size in the adhesive layer was 0.2 mm × 0.2 mm. Size grading effects were employed (bias

effect): vertically in the direction of the adhesive layer and horizontally from the inner overlap region to the overlap edges, such that a higher refinement is present at these regions. As boundary conditions, the joints were clamped at one edge and a vertical restraint and tensile displacement was applied at the opposite edge.

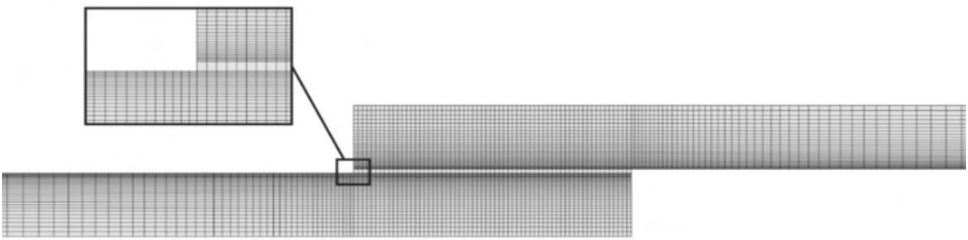

Fig. 5 – Mesh detail for the L_O=12.5 mm single-lap joint (strength prediction analysis).

4 | RESULTS

4.1 CZM law estimation by the direct method

The first step in obtaining the CZM laws of the adhesives by the direct method is the estimation of the G_I-δ_n and G_{II}-δ_s curves as described in Section 2.3 using equations and , respectively. The average values of G_{IC} and G_{IIC} were considered to build average tensile and shear CZM laws to be further applied for the strength prediction of the single-lap joints. Apart from these parameters, t_n^0 and t_s^0 are also required for the CZM laws and the average values used from the full set of CZM laws obtained from the DCB and ENF tests were as follows (in MPa): t_n^0=37.4 and t_s^0=16.8 (Araldite® AV138), t_n^0=32.9 and t_s^0=14.8 (Araldite® 2015) and t_n^0=22.0 and t_s^0=11.7 (Sikaforce® 7752). Fig. 7 depicts the t_n-d_n and t_s-δ_s curves (CZM laws) for the specimens of Fig. 6. Both tensile and shear laws of the Araldite® AV138 are best represented by a triangular approximation because of its brittleness. Oppositely, the Araldite® 2015 and Sikaforce® 7752 can be more accurately modelled with trapezoidal CZM laws because of the plasticization of these adhesives before failure.

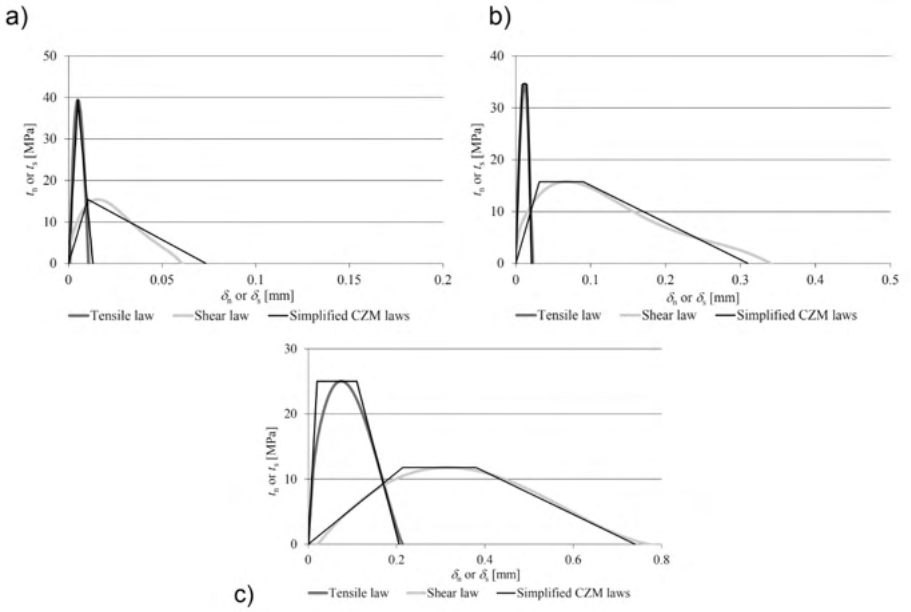

Fig. 7 – Representative t_n-δ_n and t_s-δ_s curves for the adhesives Araldite® AV138 (a), Araldite® 2015 (b) and Sikaforce® 7752 (c): obtained laws and triangular or trapezoidal approximations.

4.2 Discussion on the joint strength

Fig. 8 compares the experimental P_m values of the joints bonded with the three adhesives as a function of L_O.

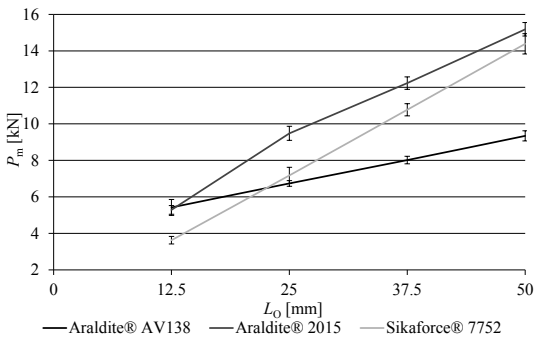

Fig. 8 – Experimental P_m-L_O curves for the adhesives Araldite® AV138, Araldite® 2015 and Sikaforce® 7752.

Different trends can be observed depending on the adhesives' strength and ductility. The value of E also has an impact on the stress distributions and thus on P_m. In fact, ADAMS (2005) concluded that smaller values of E promote more uniform stress distributions across

the bondline. Thus, the joints bonded with the Araldite® AV138 have higher peak stresses. Apart from this, peel and shear stress gradients increase for higher L_O values, resulting in P_m for higher overlaps being highly dependent on the ductility, while short overlaps are more dependent on the adhesive strength. It is also known that joints with ductile adhesives undergo plasticization at the overlap edges while the inner part of the adhesive is gradually put under loads, which promotes an increase in P_m (ADAMS; PEPPIATT, 1974). In view of this, the results of Fig. 9 show that, for L_O=12.5 mm, the high strength but brittle Araldite® AV138 results in a slightly higher value of P_m than the less strong but ductile Araldite® 2015 (experimental difference of 2.5%).

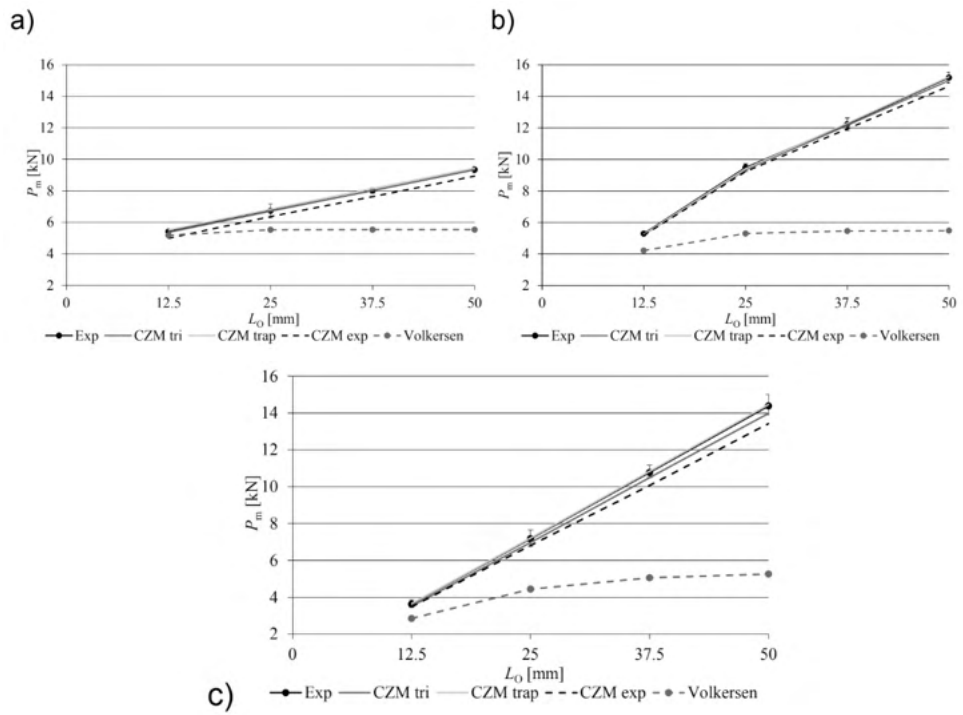

Fig. 9 – Experimental, analytical and numerical P_m-L_O curves considering triangular, trapezoidal and linear-exponential CZM laws: Araldite® AV138 (a), Araldite® 2015 (b) and Sikaforce® 7752 (c).

By increasing L_O, the higher peak stresses in the adhesive layer prevent the joints bonded with the brittle Araldite® AV138 to have a marked P_m improvement. Thus, by increasing L_O, the Araldite® 2015 gradually performs better than the Araldite® AV138 since its ductility enables plasticization after the limiting stresses are attained at the overlap edges, thus increasing t_{avg} at failure. The difference for L_O=50 mm is 62.5%. The Sikaforce® 7752 has moderate strength but extremely high ductility, which makes it fail under global yielding conditions up to large L_O values. On account of these characteristics, for small L_O values

this adhesive has the worse results since, under these conditions, failure is ruled by the adhesive strength (P_m differences, for L_O=12.5 mm, of 33.1% to the Araldite® AV138 and 31.4% to the Araldite® 2015). However, due to the largely ductile nature of this adhesive, and disregarding of the increase of peak stresses with L_O, for all tested joint configurations P_m manages to increase almost linearly with L_O. Inclusively, for L_O=50 mm, P_m is of the same order of magnitude to the Araldite® 2015 (smaller P_m by 5.3%), while higher by 54.0% over the Araldite® AV138.

4.3 Evaluation of the different CZM law shapes

Validation of the direct method for strength prediction of mixed-mode geometries was undertaken by applying the different shape CZM laws in the numerical models including CZM elements to represent failure of the adhesive layer. The average values of tensile and shear CZM parameters were used to build triangular, trapezoidal and linear-exponential tensile and shear CZM laws for each of the three adhesives. Fig. 9 presents the experimental values of P_m-L_O against the predictions for the three CZM law shapes considering the adhesives Araldite® AV138 (a), Araldite® 2015 (b) and Sikaforce® 7752 (c). A comparison to the shear-lag Volkersen's theory is also included (VOLKERSEN, 1938). Although being developed for single-lap joints, DA SILVA; DAS NEVES; ADAMS and SPELT (2009) stressed that the Volkersen's model represents better the behaviour of double-lap joints because it does not account for the bending effects induced by eccentric loads, which is less significant in double-lap joints. From the results of Fig. 9, it is found that, for the Araldite® AV138, the Volkersen's model is moderately accurate for short overlaps (error of -10.5% for L_O=12.5 mm), because of the brittleness of this adhesive that makes joints fail when the limiting stress of the adhesive is attained. However, this model fails for higher L_O values (maximum error of -40.7% for L_O=50 mm). This is because the predicted shear stresses by the Volkersen's model become constant from a certain value of L_O, which makes this model not suitable for large L_O values (DA SILVA; DAS NEVES; ADAMS; WANG*; et al.*, 2009). Oppositely to this adhesive, for the Araldite® 2015 and Sikaforce® 7752 this model highly under predicts the experimental results, since these adhesives undergo extensive plasticization prior to failure (NUNES *et al.*, 2016).

The study of CAMPILHO *et al.* (2013) for adhesive joints proved that the simulation of ductile adhesives with triangular laws results in P_m under predictions. The P_m predictions of Fig. 9 with the different law shapes show that the thin layer of Araldite® AV138 is more accurately modelled by the triangular law, with an average error of the individual errors for each L_O value of 0.4%. The trapezoidal law resulted in P_m over predictions for all L_O values, with an average difference of 1.5%. Finally, the linear-exponential law highly under estimated P_m (by an average of 5.6%). The reported results can be explained by the brittleness of the adhesive, as it can be concluded from the data of Table 1 and Fig. 7. The largest % errors always occur for L_O=12.5 mm, disregarding the CZM law type. The best predictions for the

joints bonded with the Araldite® 2015 were found by using a trapezoidal law, which is due to the moderate ductility of this particular adhesive. In this case, the average error was 0.6%, with the individual values alternating between under and over predictions, depending on L_O. The other law shapes under predicted P_m for all L_O values: in average by 1.1% for the triangular law and 2.6% for the linear-exponential law. As previously mentioned, the Sikaforce® 7752 is a highly ductile adhesive. As a consequence, also for this adhesive the trapezoidal law gives the best approximation to the experimental data (average error of 0.6%; all values by excess). The triangular and linear-exponential laws resulted in under predictions for all L_O values (in average by 2.8% for the triangular and 5.6% for the linear-exponential law). From these results, it can be found that, for the tested adhesives and geometric conditions, using an inappropriate CZM law would not result in significant errors in P_m. However, a previous work by CAMPILHO *et al.* (2013) tested triangular and trapezoidal CZM laws in single-lap joints with $10 \leq L_O \leq 80$ mm, concluding that the bigger L_O values can undergo differences of over 10% to the test results if the CZM law is not well chosen for the adhesive.

5 I CONCLUSIONS

This work aimed at the validation of the direct method for CZM law estimation of the adhesive layer in predicting the strength of single-lap joints under a tensile load, considering linear, trapezoidal and linear-exponential CZM shapes as an approximation. The tensile and shear behaviour of the Araldite® AV138 was best fit by a triangular CZM law due to its brittleness. On the other hand, the ductile Araldite® 2015 and Sikaforce® 7752 were more accurately modelled with trapezoidal CZM laws. The brittle Araldite® AV138 showed a small improvement of P_m with L_O because of the increasing stress concentrations for higher L_O values and inability of this adhesive to undergo plasticization. The moderately ductile Araldite® 2015 had a smaller P_m for the smallest L_O but, for higher L_O, revealed some ability to sustain plasticization at the overlap edges, and thus to increase strength at a higher rate than the former brittle adhesive. The highly ductile Sikaforce® 7752 failed under global yielding for all considered L_O values. Thus, because of its inferior strength, for L_O=12.5 mm, P_m was much below that of the other adhesives (for small L_O values the strengths of the adhesive rule the joint behaviour). However, for increasing L_O values, P_m of this adhesive almost matched P_m for the Araldite® 2015. The CZM predictions showed that the induced errors by using either of the CZM laws was under acceptable values (maximum average errors of 5.6% for the Araldite® AV138 and Sikaforce® 7752 by using linear-exponential CZM laws and considering all L_O values), but the best match was always attained by the previously mentioned best laws for each adhesive. As a result of these findings, it can be concluded that for the tested geometries, the CZM predictions were accurate.

REFERENCES

ABAQUS®. **Documentation of the software Abaqus®**. Dassault Systèmes. Vélizy-Villacoublay 2013.

ADAMS, R. D. **Adhesive bonding: science, technology and applications**. Cambridge, United Kingdom: Woodhead Publishing Limited, 2005.

ADAMS, R. D.; PEPPIATT, N. A. Stress analysis of adhesive-bonded lap joints. **The Journal of Strain Analysis for Engineering Design**, 9, n. 3, p. 185-196, July 1, 1974 1974.

AYDIN, M. D.; ÖZEL, A.; TEMIZ, Ş. The effect of adherend thickness on the failure of adhesively-bonded single-lap joints. **Journal of Adhesion Science and Technology**, 19, n. 8, p. 705-718, 2005/01/01 2005.

CAMPILHO, R. D. S. G.; BANEA, M. D.; NETO, J. A. B. P.; DA SILVA, L. F. M. Modelling adhesive joints with cohesive zone models: effect of the cohesive law shape of the adhesive layer. **International Journal of Adhesion and Adhesives**, 44, p. 48-56, 7// 2013.

CAMPILHO, R. D. S. G.; BANEA, M. D.; PINTO, A. M. G.; DA SILVA, L. F. M. *et al.* Strength prediction of single- and double-lap joints by standard and extended finite element modelling. **International Journal of Adhesion and Adhesives**, 31, n. 5, p. 363-372, 7// 2011.

CAMPILHO, R. D. S. G.; MOURA, D. C.; BANEA, M. D.; DA SILVA, L. F. M. Adhesive thickness effects of a ductile adhesive by optical measurement techniques. **International Journal of Adhesion and Adhesives**, 57, p. 125-132, 3// 2015.

CONSTANTE, C. J.; CAMPILHO, R. D. S. G.; MOURA, D. C. Tensile fracture characterization of adhesive joints by standard and optical techniques. **Engineering Fracture Mechanics**, 136, p. 292-304, 3// 2015.

DA SILVA, L. F. M.; DAS NEVES, P. J. C.; ADAMS, R. D.; SPELT, J. K. Analytical models of adhesively bonded joints—Part I: Literature survey. **International Journal of Adhesion and Adhesives**, 29, n. 3, p. 319-330, 4// 2009.

DA SILVA, L. F. M.; DAS NEVES, P. J. C.; ADAMS, R. D.; WANG, A. *et al.* Analytical models of adhesively bonded joints—Part II: Comparative study. **International Journal of Adhesion and Adhesives**, 29, n. 3, p. 331-341, 4// 2009.

FLOROS, I. S.; TSERPES, K. I.; LÖBEL, T. Mode-I, mode-II and mixed-mode I+II fracture behavior of composite bonded joints: Experimental characterization and numerical simulation. **Composites Part B: Engineering**, 78, p. 459-468, 9/1/ 2015.

JI, G.; OUYANG, Z.; LI, G.; IBEKWE, S. *et al.* Effects of adhesive thickness on global and local Mode-I interfacial fracture of bonded joints. **International Journal of Solids and Structures**, 47, n. 18–19, p. 2445-2458, 9// 2010.

JUMEL, J.; BEN SALEM, N.; BUDZIK, M. K.; SHANAHAN, M. E. R. Measurement of interface cohesive stresses and strains evolutions with combined mixed mode crack propagation test and Backface Strain Monitoring measurements. **International Journal of Solids and Structures**, 52, p. 33-44, 1/1/ 2015.

LEFFLER, K.; ALFREDSSON, K. S.; STIGH, U. Shear behaviour of adhesive layers. **International Journal of Solids and Structures**, 44, n. 2, p. 530-545, 1/15/ 2007.

LEITÃO, A. C. C.; CAMPILHO, R. D. S. G.; MOURA, D. C. Shear Characterization of Adhesive Layers by Advanced Optical Techniques. **Experimental Mechanics**, p. 1-14, 2015/12/02 2015.

LOUREIRO, A. L.; DA SILVA, L. F. M.; SATO, C.; FIGUEIREDO, M. A. V. Comparison of the Mechanical Behaviour Between Stiff and Flexible Adhesive Joints for the Automotive Industry. **The Journal of Adhesion**, 86, n. 7, p. 765-787, 2010/07/16 2010.

NUNES, S. L. S.; CAMPILHO, R. D. S. G.; DA SILVA, F. J. G.; DE SOUSA, C. C. R. G. *et al.* Comparative failure assessment of single and double-lap joints with varying adhesive systems. **The Journal of Adhesion**, 92, p. 610-634, 2016.

PANDYA, K. C.; WILLIAMS, J. G. Measurement of cohesive zone parameters in tough polyethylene. **Polymer Engineering & Science**, 40, n. 8, p. 1765-1776, 2000.

TURON, A.; DÁVILA, C. G.; CAMANHO, P. P.; COSTA, J. An engineering solution for mesh size effects in the simulation of delamination using cohesive zone models. **Engineering Fracture Mechanics**, 74, n. 10, p. 1665-1682, 7// 2007.

VALOROSO, N.; SESSA, S.; LEPORE, M.; CRICRÌ, G. Identification of mode-I cohesive parameters for bonded interfaces based on DCB test. **Engineering Fracture Mechanics**, 104, p. 56-79, 5// 2013.

VOLKERSEN, O. Die nietkraftoerteilung in zubeanspruchten nietverbindungen mit konstanten loschonquerschnitten. **Luftfahrtforschung**, 15 p. 41-47, 1938.

ZHU, Y.; LIECHTI, K. M.; RAVI-CHANDAR, K. Direct extraction of rate-dependent traction–separation laws for polyurea/steel interfaces. **International Journal of Solids and Structures**, 46, n. 1, p. 31-51, 1/1/ 2009.

ÍNDICE REMISSIVO

A

Acai berry 74

Accessibility 2, 32, 140

Adaptability 112

Adhesive joints 126, 136, 138, 139

Advertisement videos 96

Animals 2

Aquaculture reproduction 48

Arduino 2, 4, 5, 12, 47, 49, 52, 57, 61, 74, 77, 80, 82

Autistic spectrum disorder 32, 140

Automated monitoring 47, 48

Automation 74, 191

Automation software 191

C

Clustering 14, 15, 29, 30, 31

Cognition 111, 112

Cohesive zone models 126, 138, 139

Compilers 84

Cyber-crime 169

D

Data science 15

Digital image correlation 126, 128, 130

Digital TV 84, 94

E

Emotional branding 95, 96, 99, 101, 102, 108

Employers 116

F

Feature extraction 15

Final project report 191

Finite element method 126, 127

G

Geovisualization 111, 112

Gestión de riesgos 63, 65, 68, 69, 70, 71

Gestión proyecto 152

Graduates 116

I

Informática 11, 30, 46, 63, 65, 77, 82, 94, 152, 169, 170, 171, 172, 187, 189

Information technologies 191

Innovation 74, 110

Interface 4, 32, 33, 35, 36, 38, 40, 45, 52, 76, 112, 114, 115, 128, 138, 140, 141, 143, 144, 145, 146, 149, 150, 175, 177, 178, 180, 185, 186

M

Machine learning technique 47, 48

Máquinas de guerra 209, 214, 215

Migración sistema legado 152

N

Narrativas acadêmicas 209

Neuromarketing 95, 96, 98, 99, 101, 102, 107, 108, 109, 110

P

Panvel Pharmacy 96

PEG 84, 89

Prototype 2, 74, 140

R

Retail 63, 64, 65, 69, 71

Rootkit 169, 170, 180, 184, 185, 186, 188

S

Scouts 74

Seguridad informática 63, 65

Sistema bedelías 152

Sistema de gestión de la enseñanza 152

Sistema misión crítica 152

Structural adhesives 126, 127, 128

U

Usability assessment 32

V

Virtual learning space 191

www.atenaeditora.com.br
contato@atenaeditora.com.br
@atenaeditora
www.facebook.com/atenaeditora.com.br

Collection:

APPLIED COMPUTER ENGINEERING

Atena Editora
Ano 2022

www.atenaeditora.com.br
contato@atenaeditora.com.br
@atenaeditora
www.facebook.com/atenaeditora.com.br

Collection:

APPLIED COMPUTER ENGINEERING

Atena Editora
Ano 2022